Endocranial morphology of *Pygoscelis calderensis* (Aves, Spheniscidae) from the Neogene of Chile and remarks on brain morphology in modern *Pygoscelis*

Ariana Paulina-Carabajal[a,b]*, Carolina Acosta-Hospitaleche[a,c] and Roberto E. Yury-Yáñez[d]

[a]*Consejo Nacional de Investigaciones Científicas y Técnicas, Buenos Aires, Argentina;* [b]*Museo Carmen Funes, Av. Córdoba 55 (8318) Plaza Huincul, Neuquén, Argentina;* [c]*División Paleontología de Vertebrados, Museo de la Plata, Paseo del Bosque s/n, 1900 La Plata, Argentina;* [d]*Laboratorio de Zoología de Vertebrados, Departamento de Ciencias Ecológicas, Facultad de Ciencias, Universidad de Chile, Las Palmeras 3425, Ñuñoa, Santiago de Chile, Chile*

(*Received 22 January 2014; accepted 21 February 2014*)

The endocranial anatomy of *Pygoscelis calderensis*, a fossil species from the Bahía Inglesa Formation (Middle Miocene–Pliocene) of Chile, South America, was described through CT scans. Reconstructions of the fossil *P. calderensis* and endocasts for the living *Pygoscelis adeliae*, and *Pygoscelis papua* are provided here for the first time. Comparisons with the extant congeneric species *P. adeliae*, *Pygoscelis antarctica* and *P. papua* indicate that the morphological pattern of the brain and inner ear of the extant pygoscelids has been present already in the Middle Miocene. The neurological morphology suggests that the paleobiology of the extinct form would have been similar to the extant species. It was probably true for diet, feeding behaviour and diving kinematics.

Keywords: braincase; cranial endocast; inner ear; *Pygoscelis*; South America

1. Introduction

Fossil penguins are well known in the Cenozoic levels of southern South America. According to the fossil record, the Neogene was an important time for penguin diversity and abundance (e.g. Acosta Hospitaleche et al. 2007, 2008; Stucchi 2007; Rubilar-Rogers et al. 2012). Nevertheless, the intrinsic features of the weak skull bones make the preservation of cranial elements very unlikely. Consequently, cranial remains are not common in the record, and anatomical descriptions of fossil penguin neuroanatomy are scarce. For example, some brain information was published for *Spheniscus magellanicus* (Bee de Speroni and Pirlot 1987), and a complete cranial endocast referable to an extinct species of cf. *Spheniscus* was mentioned for the late Miocene of Chile (Walsh 2001). Recently, the neuroanatomy of *Paraptenodytes antarcticus* was studied by Ksepka et al. (2012), also including the endocranial reconstructions of the extant species *Aptenodytes patagonicus* (King Penguin), *Spheniscus humboldti* (Humboldt Penguin) and *Pygoscelis antarctica* (Chinstrap Penguin).

The genus *Pygoscelis* is currently represented by three species: *Pygoscelis adeliae*, *P. antarctica* and *Pygoscelis papua*, and three Mio-Pliocene representatives: (1) the New Zealander *Pygoscelis tyreei* Simpson, 1972, whose taxonomic generic assignment is debatable; (2) the Chilean *Pygoscelis grandis* Walsh and Suárez, 2006, described from postcranial remains and (3) the Chilean *Pygoscelis calderensis* (Acosta Hospitaleche et al. 2006), known only through a few skulls. The diagnosis of *P. calderensis* is entirely based on external cranial morphology (Acosta Hospitaleche et al. 2006); and the cranial anatomy of the genus *Pygoscelis* has been widely studied (Acosta Hospitaleche and Tambussi 2006; Acosta Hospitaleche et al. 2006). However, the endocranium (brain and inner ear) remains poorly studied, except for *P. antarctica*, whose brain morphology was described by Ksepka et al. (2012).

Here, we present a paleoneurological study of *P. calderensis* focused on the exploration of endocranial characters of the extinct species and its modern representatives *P. adeliae*, *P. antarctica* and *P. papua*. CT scan data of *P. calderensis* and the three living species of the genus were compared in order to find features that shed some light on the understanding of the paleobiology of the extinct species.

2. Materials and methods

Fossil remains here presented are from the phosphatic levels of the Bahía Inglesa Formation, assigned to the Middle Miocene according to micropaleontological studies (Marchant et al. 2000; Achurra Reveco 2004). They are permanently housed at the Museo Nacional de Historia Natural (SGO PV) of Santiago de Chile (Chile), whereas the modern specimens belong to the collections of the División Paleontología de Vertebrados of the Museo de La Plata (MLP), La Plata (Argentina).

The three fossil braincases of *P. calderensis* (SGO PV 790, SGO PV 791 and SGO PV 792) from the Bahía

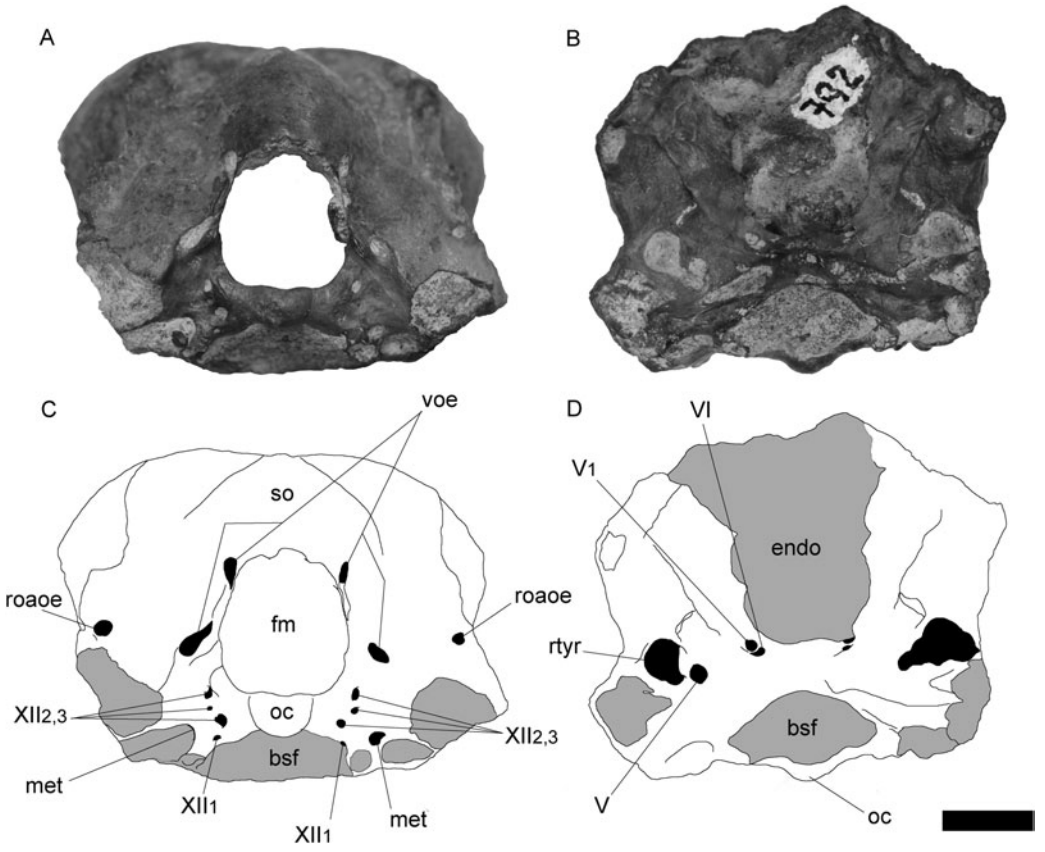

Figure 1. Photographs (A and B) and line drawings (C and D) of the braincase of *P. calderensis* (SGO PV 792) in posterior (A and C) and ventral (B and D) views. bsf, basisphenoid; endo, endocranial cavity; fm, foramen magnum; met, metotic foramen (CNs IX–XI); oc, occipital condyle; roaoe, foramen *rami occipitalis arteriae ophthalmicae externae*; rtyr, rostral tympanic recess; so, supraoccipital; voe, *vena occipitalis externa*; V, trigeminal nerve (V_1, ophthalmic branch); XII, hypoglossal nerve. Scale bar = 1 cm.

Inglesa Formation (Los Dedos locality, Atacama Region, Chile) and Antarctic representatives of the three living species of the genus (*P. adeliae* MLP 464, *P. antarctica* MLP 470 and *P. papua* MLP 38) were CT-scanned and reconstructed. CT scans of *P. calderensis* were performed at Fundación Arturo Lopez Pérez, Santiago de Chile (Chile), using a Toshiba Aquilion 64 channels, multi-detector tomographer, while a Philips Brilliance, 64-channel CT multislice tomographer was used for the extant species in La Plata (Argentina). The slices were taken at 0.63-mm intervals. Virtual three-dimensional inner ear and cranial endocasts were obtained using the software Mimics (version 14.0) and Geomagic at the University of Alberta Paleovertebrate Laboratory (Canada).

As in many other adult birds, the braincase and skull roof elements of the three specimens of *P. calderensis* are firmly fused and there are no visible sutures. The general description is focused on the brain and inner ear virtual endocasts of the three specimens of *P. calderensis* (although the reconstruction is complete, most of the anterior cranial nerves (CNs) and vascular elements are not shown) and the three living species of *Pygoscelis*. Anatomical terminology used for the braincase description follows the Nomina Anatomica Avium (Baumel et al. 1993). The most complete digital endocranial reconstructions of *P. calderensis* correspond to the specimen SGO PV 791.

3. Results and discussion

3.1 Braincase CN and vascular foramina

On the occipital plate, the foramen magnum is largely circumscribed dorsolaterally by the supraoccipital (Figure 1(A),(C)). The lateroventral expansions of the supraoccipital overhang laterodorsally a small slit on each side of the foramen magnum, which is part of a well-marked groove, probably for the first pair of spinal nerves. Laterodorsally to the foramen magnum, there is a foramen for the *vena occipitalis externa* (= caudal middle cerebral vein). The foramen is located at the dorsal distal end of an elongated and vertical groove.

Lateral to the groove for the *vena occipitalis externa*, there is a large circular foramen bounded between the nuchal crest and the paroccipital process that corresponds

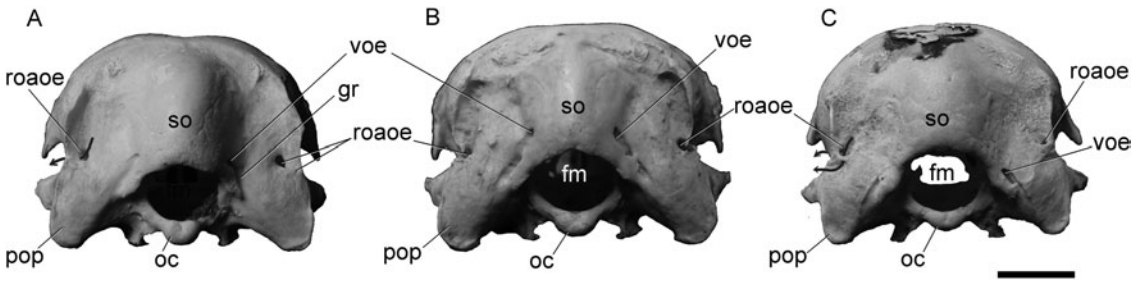

Figure 2. Braincase of *P. antarctica* (A), *P. adeliae* (B) and *P. papua* (C) in posterior view. fm, foramen magnum; pop, paroccipital process; oc, occipital condyle; so, supraoccipital; voe, *vena occipitalis externa*; roaoe, foramen *rami occipitalis arteriae ophthalmicae externae*. Scale bar = 1 cm.

to the foramen *rami occipitalis arteriae ophthalmicae externae*, which is not connected with the endocranial cavity (Figure 1(B)). This foramen is related with a smaller foramen that faces laterally in all the studied species except in *P. adeliae*. In the last taxon, the lateral margin of the foramen *rami occipitalis arteriae ophthalmicae externae* is not ossified, and the smaller foramen observed in the other species is not present (Figure 2(B)). The vascular element then pierces the nuchal crest and runs from the occiput anteroventrally – dorsal to the paroccipital process – to pierce the squamosal ventrally and entering the condylar facet for the quadrate (*cotyla quadratica squamosi*) (Figure 3).

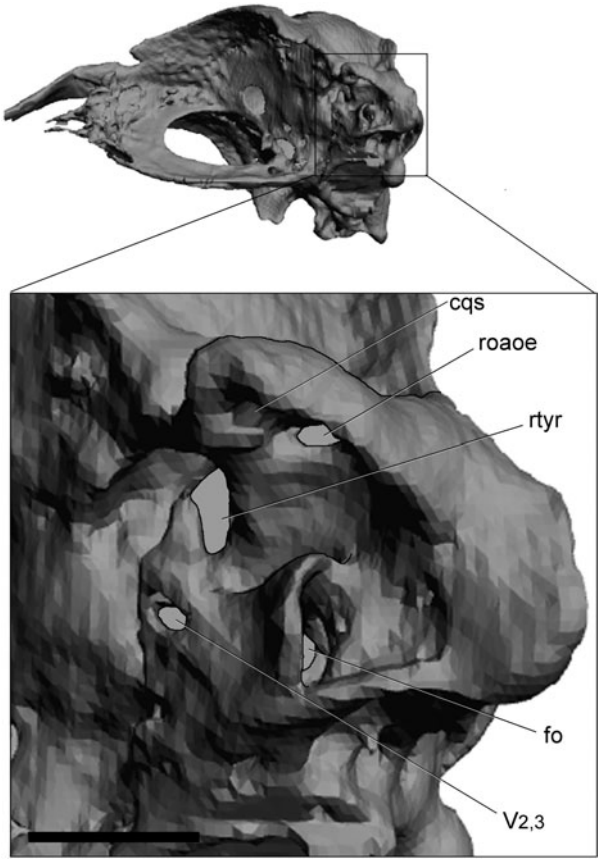

Figure 3. Volume-rendered CT-based reconstruction of the skull of *P. antarctica*. Detail of middle ear region. cqs, *cotila quadratic squamosi*; eu, Eustachian tube; fo, *fenestra ovalis*; roaoe, foramen for the ventral ramus of *rami occipitalis arteriae ophthalmicae externae*; rtyr, rostral tympanic recess; $V_{2,3}$, foramen for the trigeminal maxillar and mandibular branches. Scale bar = 1 cm.

In *P. calderensis*, there are four foramina for CN XII lateroventral to the *condylus occipitalis*, as in *P. adeliae* (Figures 1(A) and 2(A)–(C)). In the last taxon, the dorsal foramen for CN $XII_{2,3}$ is divided by a bony bridge, resulting in a total of four external cranial foramina for the branches of this nerve. The dorsal foramen for CN $XII_{2,3}$ has a median constriction separating two lobes in *P. antarctica* and *P. papua*, and located lateral to the neck of the condyle, whereas the markedly smaller foramen located ventrally and near the posterior margin of the basal tuber corresponds to CN XII_1. Anterior to the mentioned foramina and below the paroccipital process, there are two foramina for CN IX–XI, the largest foramen probably for CN X–XI, whereas the smallest, located posterior to the larger internal carotid foramen, corresponds to a separated branch of CN XI (Figure 4). A third passage for CN IX–XI is entering the tympanic cavity and therefore its exit foramen is not observed externally on the braincase. Endocranially, however, there is a single foramen for CN IX–XI in all the species except for *P. adelia*, in which there are two foramina, the smallest also leading to the tympanic cavity.

The internal carotid artery foramen is the largest one on the occipital plate. It opens within a shallow oval recess anterior to the CN X foramen and ventral to the paroccipital process. The internal carotid passage is completely enclosed in bone and runs anteromedially through the basisphenoid, below the Eustachian tube, to enter the pituitary fossa.

As mentioned by Saiff (1976), the penguin middle ear is characterised by a conical tympanic cavity, with the external auditory canal directed posteroventrally. Deep inside the cavity, three large fenestrae are recognised in the living *Pygoscelis*. On the medial wall of the tympanic

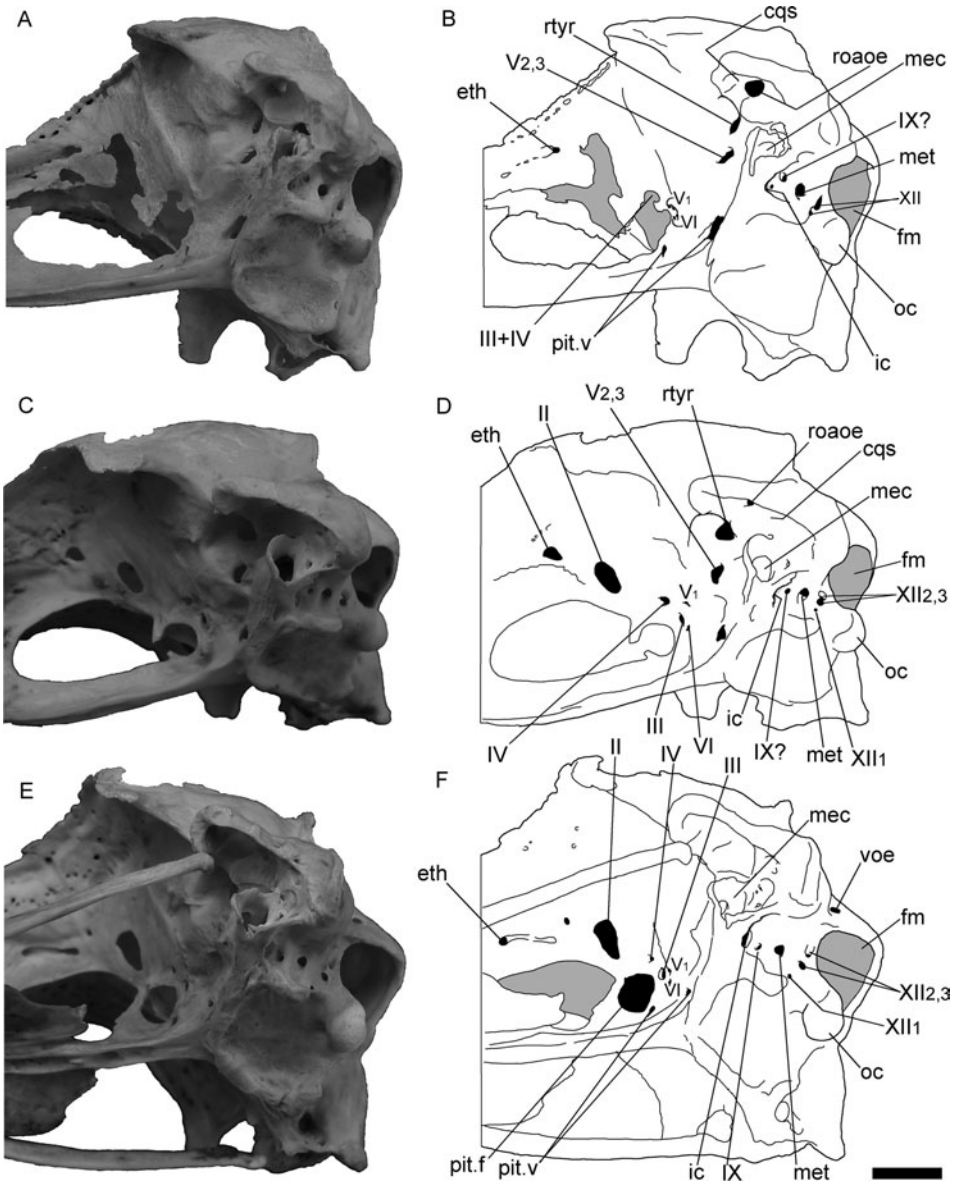

Figure 4. Photographs (A, C and E) and line drawings (B, D and F) of the braincases of *P. papua* (A and B), *P. antarctica* (C and D) and *P. adeliae* (E and F) in right lateroventral views. eth, vascular element of the ethmoidal region; ic, internal carotid artery foramen; mec, middle ear cavity; met, metotic foramen (CNs IX–XI); oc, occipital condyle; pit.f, pituitary anterior fenestra; pit.v, pituitary vascular foramen; pop, paroccipital process; roaoe, foramen *rami occipitalis arteriae ophthalmicae externae*; rtyr, rostral tympanic recess; voe, *vena occipitalis externa*; II–XII, CNs. Scale bar = 1 cm.

cavity and posteriorly located is the large oval *fenestra ovalis* (Figure 3). Posteroventrally to the *fenestra ovalis*, excavated on the posterior wall of the cavity, there is a large fenestra that communicates dorsally with a pneumatic cavity within the paroccipital process, and posteriorly with the endocranial cavity through a passage for one of the CN IX–XI (probably CN IX). This is the case for *P. antarctica*, and *P. papua*, whereas in *P. adeliae* there are two CN passages entering into the tympanic cavity as mentioned above. Finally, on the posteroventral wall of the tympanic cavity opens the Eustachian tube, which runs anteromedially to converge with its counterpart below the pituitary fossa. Saiff (1976) also describes the hyomandibular branch of CN VII exiting through a foramen located posterodorsal and lateral to the *fenestra ovalis* that 'leaves the middle ear region with the stapedial artery through the stapedial foramen'. In the case of the living *Pygoscelis*, the small foramen that we identify as the hyomandibular branch of CN VII is anterodorsal to the *fenestra ovalis*. The passage for this branch seems to be connected with the palatine branch passage, which opens laterally on the braincase, posterodorsal to CN $V_{2,3}$.

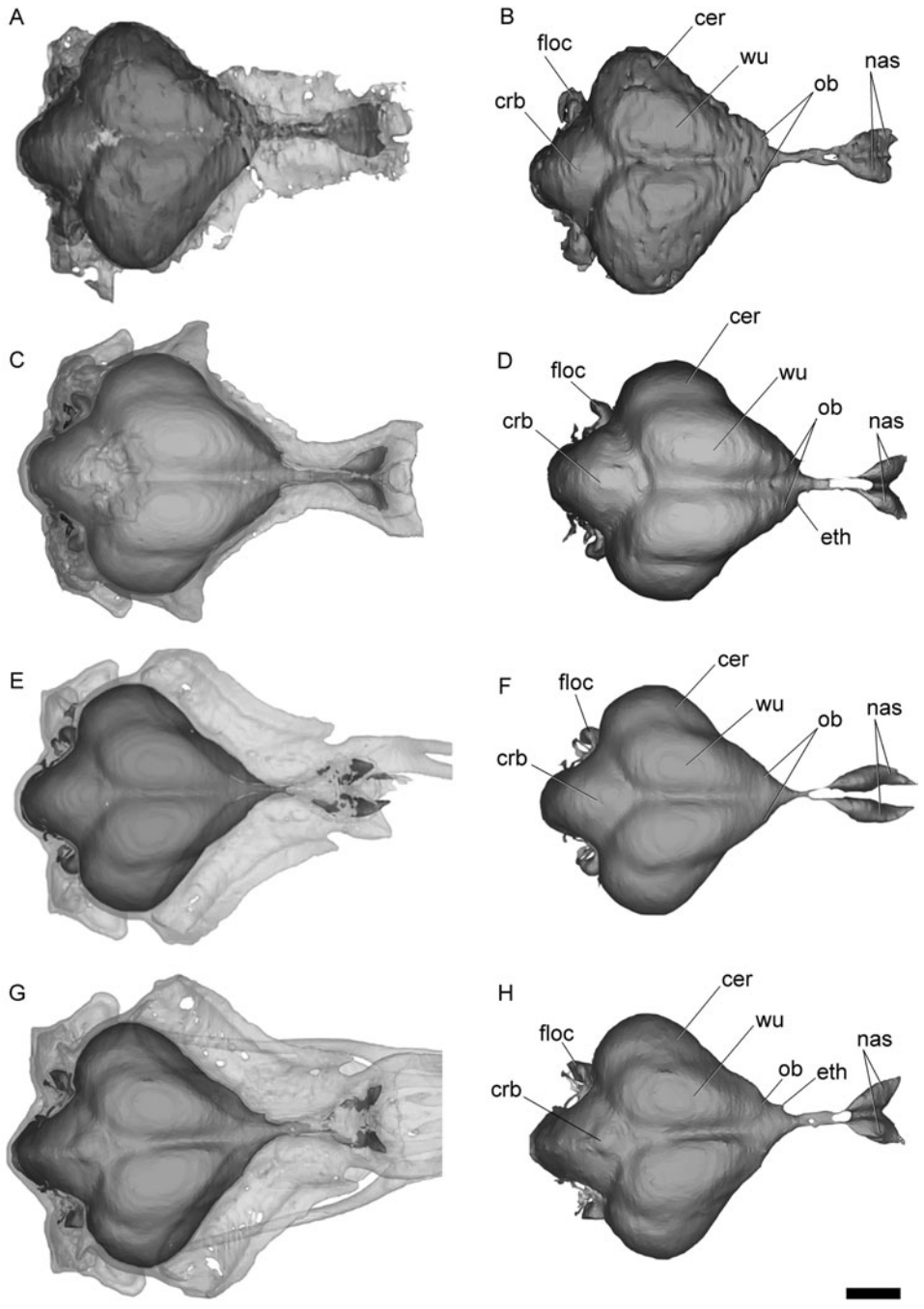

Figure 5. Volume-rendered CT-based reconstruction of the skull and brain of *Pygoscelis* species in dorsal view. In the images on the left, the bone is rendered semitransparent to show the endocranial cast. *P. calderensis* (A and B), *P. papua* (C and D), *P. antarctica* (E and F) and *P. adeliae* (G and H).cer, cerebral hemisphere; crb, cerebellum; eth, ethmoidal vasculature; floc, flocculus (*auricula cerebelli*); nas, nasal cavity; ob, olfactory bulb; wu, wulst. Scale bar = 1 cm.

Unfortunately, because of the small diameter of the two passages, CN VII is not reconstructed on the digital endocast.

The foramen for CN $V_{2,3}$ is large and located dorsal to the basipterygoid process in *P. antarctica* and *P. adeliae*, whereas the two branches (CN V_2 and CN V_3) are separated by a small ridge of bone in *P. papua*. The markedly small ophthalmic branch (CN V_1) foramen is widely separated and opens anteroventrally, just behind the posterior margin of the pituitary fenestra in all the living species (Figure 4(B),(D) and (F)). Anteroventral to CN V_1 is the even smaller foramen for CN VI, which is enclosed by the basisphenoid, indicating the contact between this bone and the laterosphenoid. In *P. adeliae* and

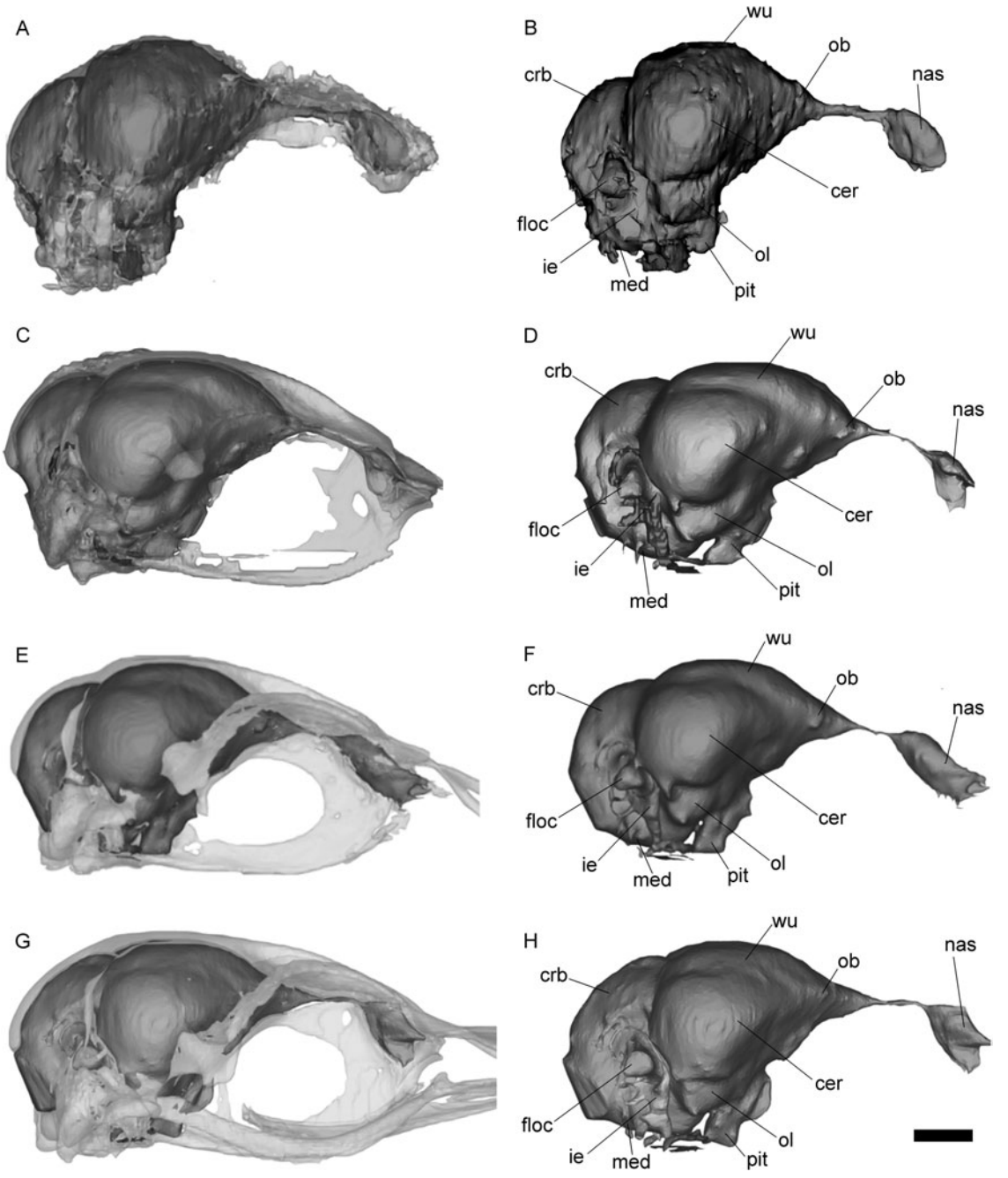

Figure 6. Volume-rendered CT-based reconstruction of the skull and brain of *Pygoscelis* species in right lateral view. In the images on the left, the bone is rendered semitransparent to show the endocranial cast. *P. calderensis* (A and B), *P. papua* (C and D), *P. antarctica* (E and F) and *P. adeliae* (G and H). cer, cerebral hemisphere; crb, cerebellum; ie, inner ear; med, medulla; nas, nasal cavity; ob, olfactory bulb; ol, olfactory lobe; pit, pituitary; wu, wulst. Scale bar = 1 cm.

P. antarctica, there are two circular foramina lateral to the pituitary opening for CN III and CN IV, whereas in *P. papua*, both foramina are confluent in a single elongated opening (Figure 4(B)). CN II is the largest foramen in the braincase and is widely separated from its counterpart. Between these and the pituitary opening, there is a small pair of foramina located close to the midline that corresponds probably to a vascular element related to the pituitary gland region.

The rostral middle cerebral vein (and probably also the dorsal head vein) exits the endocranial cavity through the rostral tympanic recess (*foramen pneumaticum dorsale* in Bertelli et al. 2006). This recess is largely excavated dorsal to CN V and anterior to the *cotyla*

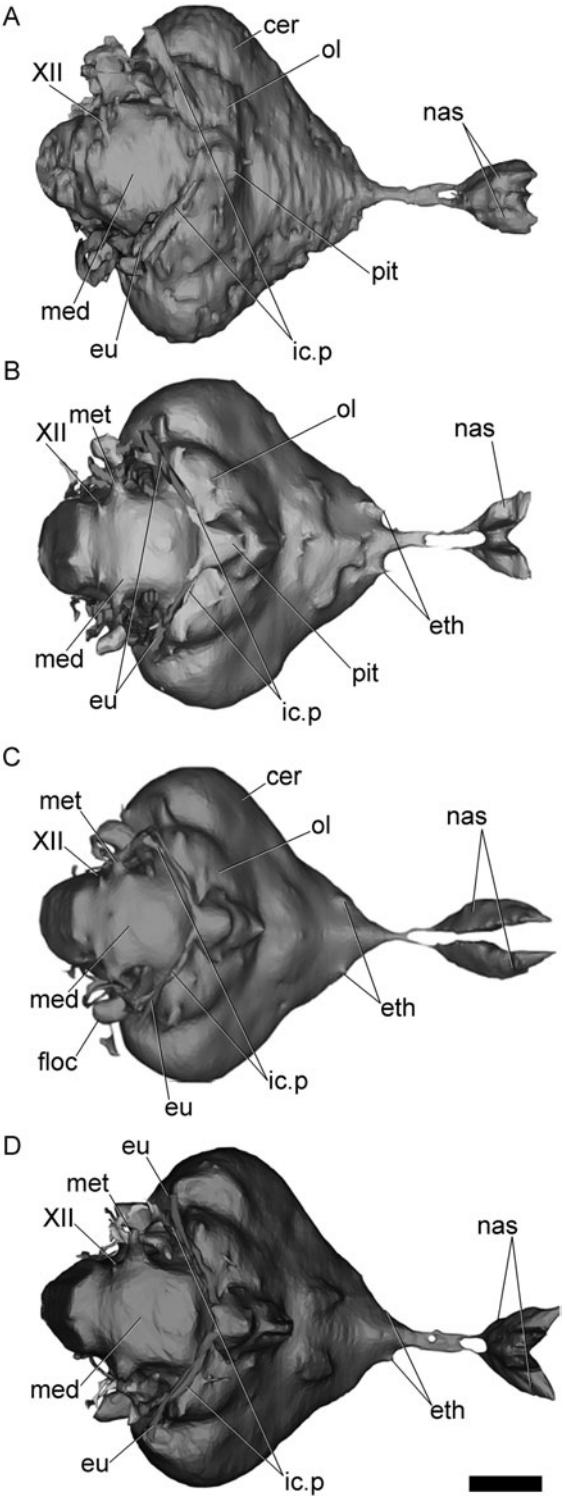

Figure 7. Volume-rendered CT-based reconstruction of brain of *P. calderensis* (A), *P. papua* (B), *P. antarctica* (C) and *P. adeliae* (D) in ventral view. cer, cerebral hemisphere; eth, ethmoidal vasculature; eu, Eustachian tube; floc, flocculus (*auricula cerebelli*); ic.p, internal carotid artery passage; med, medulla; met, metotic passage for CN IX–XI; nas, nasal cavity; ol, optic lobe; pit, pituitary; XII, hypoglossal nerve. Scale bar = 1 cm.

quadratica squamosi, and is better observed in lateroventral or ventral view of the braincase (Figure 3).

Anterodorsal to CN II, enclosed by the ethmoidal elements and near the contact with the frontal, there is a pair of vascular foramina. They are associated internally with the olfactory bulbs and the base of the nasal canal and cavity. Variation in the configuration of these foramina was found between different species: for example, while the anterior foramen is continuous with an anteroposterior groove in *P. adeliae* (Figure 4(F)), in *P. papua* both foramina are confluent (Figure 4(B)).

3.2 *Brain morphology*

The morphology of the cranial endocast and inner ear of *P. calderensis* is very similar to that observed in other congeneric penguins (Figures 5–8). The modern species are truly similar to *Pygoscelis* sp., in which the brain is oriented mainly parallel to the main axis of the skull, as described for other extinct and extant penguins (see Ksepka et al. 2012).

3.2.1 *Forebrain*

Virtual digital reconstruction of the forebrain includes the olfactory bulbs (CN I), cerebral hemispheres, optic nerves (CN II) and the pituitary body. As mentioned by Ksepka et al. (2012), the pineal gland (between the cerebellar and cerebral hemispheres) does not leave a visible impression on the endocranial cavity and therefore on the endocast.

In all the taxa analysed here, the olfactory tract and bulbs are anteriorly projected from the cerebral hemispheres. The olfactory tract is extremely short and the olfactory bulbs are oval-shaped and slightly divergent from the midline. Anteriorly to the olfactory bulbs, there is a pair of nasal ducts running anteroventrally towards large and oval nasal cavities (Figure 5(B),(D),(F)–(H)). Ksepka et al. (2012) reported low olfactory ratios (greatest linear dimension of the olfactory bulb divided by the greatest linear dimension of the cerebral hemispheres) in *P. adeliae*. Based on the similar proportions observed in the brain of the other species of *Pygoscelis*, we assumed that this would be also true for *P. antarctica*, *P. papua* and the fossil *P. calderensis*.

The maximum width of the endocranial cast corresponds to the cerebral hemispheres (Table 1). Each cerebral hemisphere is markedly expanded laterally occluding the optic lobe in dorsal view, as in most living birds (Milner and Walsh 2009; Walsh and Milner 2011a, 2011b). As mentioned by Ksepka et al. (2012), the cerebral hemispheres of all sampled penguins have a 'heart-shaped' appearance in dorsal view (Figure 5). The *fisura interhemispheria* is a deep straight longitudinal groove separating the cerebral hemispheres medially. Dorsally,

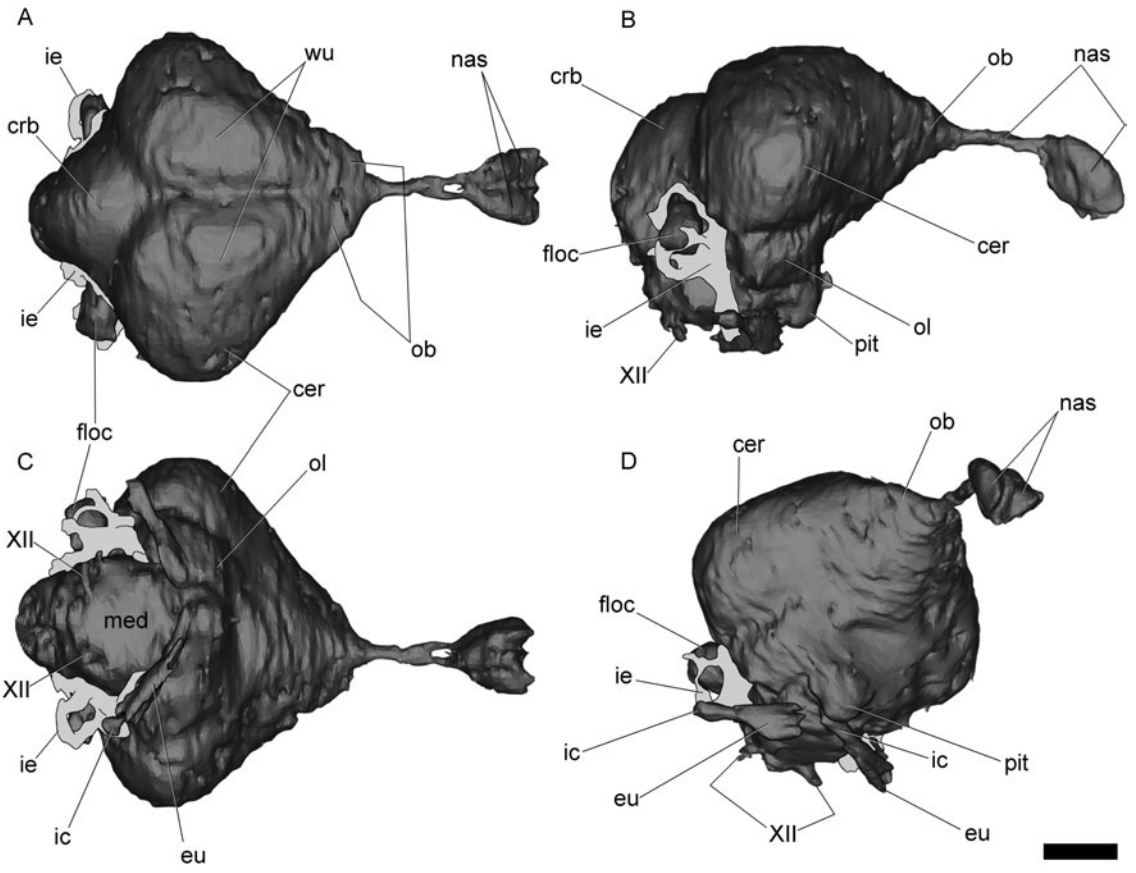

Figure 8. Brain morphology of *P. calderensis* in dorsal (A), lateral (B), ventral (C) and right lateroventral (D) views. cer, cerebral hemisphere; crb, cerebellum; eu, Eustachian tube; ic, internal carotid passage; ie, inner ear; ob, olfactory bulb; ol, optic lobe; floc, flocculus (*auricula cerebelli*); med, medulla; nas, nasal cavity; pit, pituitary; wu, wulst; XII, hypoglossal nerve. Scale bar = 1 cm.

there is an evident *eminentia sagittalis* or wulst as in other penguin genera such as *Aptenodytes* and *Spheniscus* among living forms, and *Paraptenodytes* among fossil taxa (Bee de Speroni and Pirlot 1987; Ksepka et al. 2012). The *eminentia sagittalis* is sub-elliptically shaped in dorsal view and is separated from the rest of the hemispherium by a conspicuous vallecula. For further discussion on the significance of the development of the wulst in birds, see Ksepka et al. (2012).

The pituitary body, also part of the diencephalon, descends from the ventral surface of the endocast and exhibits a pyramidal shape (Figures 6 and 7). The internal carotid arteries enter the pituitary fossa posteriorly, just after forming a small anastomosis (Figure 7). From the three types of anastomosis recognised in birds (see Baumel and Gerchman 1968), we identified the 'x-type' in the living species *P. antarctica*, *P. adeliae* and *P. papua*, and in the fossil *P. calderensis* (Figures 7 and 9).

Table 1. Endocranial measurements (in mm) of *Pygoscelis* genera.

	Brain measurements				Inner ear measurements			
Taxon	L1	L2	Cer	Wu	L	asc	psc	lsc
P. adeliae	71.2	49.4	47.5	33.0	21.3	11.5	7.0	5.5
P. antarctica	67.0	43.7	41.0	26.5	19.5	9.0	7.0	4.5
P. calderensis (SGOPV 791)	66.5	45.5	45.5	27.0	21.0	8.2	6.3[a]	5.5
P. papua	73.0	53.5	49.5	33.6	23.3	11.0	7.0	4.5

Note: Cer, maximum width of brain through cerebral hemispheres; L, Length; L1, Length of the brain including nasal cavities; L2, Length of the brain excluding nasal ducts and cavities; asc, internal maximum diameter of anterior semicircular canal; psc, internal maximum diameter of posterior semicircular canal; lsc, internal maximum diameter of lateral semicircular canal; Wu, maximum width of brain through the wulst.
[a] Incomplete measurement.

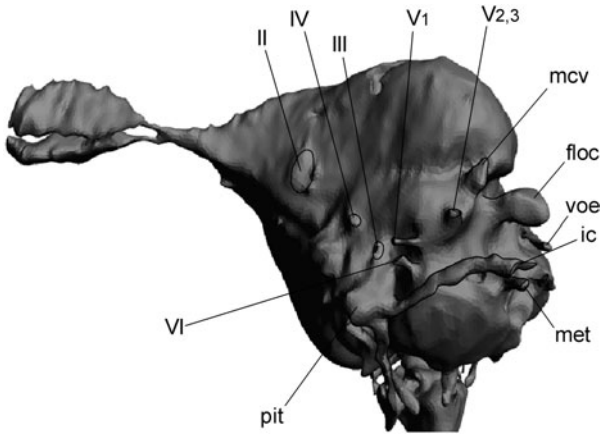

Figure 9. Surface-rendered CT-based reconstruction of the cranial endocast of *P. antarctica* in left lateroventral view. ic, internal carotid passage; ol.v, olfactory vein; floc, floccular process (auricular cerebelli); med, medulla; met, metotic passage (CN IX–XI); nas, nasal cavity; pit, pituitary; mcv, rostral middle cerebral vein; voe, vena occipitalis externa. Not to scale.

In the modern species, there is a small pituitary vein exiting anterolaterally the pituitary fossa. Dorsally, there is one (*P. papua*) or two (*P. adeliae* and *P. antarctica*) vascular elements on the sphenoidal region, clearly associated with the olfactory bulb and the nasal conduct (Figure 7).

As in other birds, the olfactory tract is extremely short and the olfactory bulbs are small and not clearly differentiated from the forebrain (Figures 5 and 8). In front of the olfactory bulb runs a 'nasal conduct' that ends in large paired oval nasal cavities. CN I is represented by the olfactory tract and olfactory bulbs in the endocasts. As mentioned above, the size of the olfactory bulbs suggests a low olfactory ratio for extinct and living species.

CNs II (optic nerves) exit the endocranial cavity through a pair of large, circular foramina enclosed by the orbitosphenoids, which are transversely separated by an osseous bridge. None of the fossil specimens show complete margins for CN II (Figure 1(B)).

3.2.2 *Midbrain*

The visible mesencephalic structures in the cranial endocast consist of the optic lobes and CNs III and IV. The optic lobes are relatively well developed as in other living and extinct birds (Walsh and Milner 2011a, 2011b) and posteroventrally located regarding the cerebral hemispheres (Figure 8(B),(C)). Ksepka et al. (2012) stated that the amount of variation in the form of the optic lobe within Spheniscidae is small compared with that between penguins and other groups.

Endocranially, CNs III and IV are located laterally to the infundibulum. In *P. antarctica* and *P. adeliae*, CNs III and IV are separated from each other being similar in diameter. In *P. papua*, the foramina for CN III and CN IV are confluent. In the braincase, the medial margins of both foramina are not completely ossified.

3.2.3 *Hindbrain*

The visible features in this region of the cranial endocast include the cerebellum, the medulla oblongata and CNs V–XII. The medulla oblongata is elongated and its ventral surface presents a rostro-caudally oriented mark that we interpret as a blood vessel. The cerebellum is globose and largely exposed in dorsal view as in other birds (Figures 5 and 8(A)). The *auricula cerebelli* (= floccular process) is large, and closely related to the anterior semicircular canal of the inner ear (Figures 6, 8 and 9). Endocranially, the *auricula cerebelli* is hosted within a large recess, the *fossae auriculae cerebelli*. The size of the fossa is similar to that in other diving birds (Elzanowski and Galton 1991), indicating that penguins did not lose the 'flying' characteristics observed in the brain, as pointed out by Ksepka et al. (2012).

CN $V_{2,3}$ has a large foramen and an extremely short passage in the braincase (Figures 4 and 9). In all the species examined here, the ophthalmic branch of the trigeminal nerve is separated and exits the braincase through a small foramen located posterodorsally but near to CN VI. In *P. antarctica* and *P. adeliae*, the maxillary and palatine branches (CN $V_{2,3}$) exit the braincase through a single foramen, whereas in *P. papua* the foramen is divided by an osseous septum. This is not observed in the virtual endocast.

In the braincase of the three living species of *Pygoscelis*, the foramen of CN VI is located anteroventrally to the ophthalmic branch (CN V_1). In the endocasts of the living species, CN VI has a short passage of small diameter that runs from the floor of the medulla oblongata to exit the braincase posteroventrally to CN III–IV (Figures 4 and 9). This disposition of the CNs is probably also present in the extinct form.

CN VII is small, and the external foramen in the braincase is posterior to CN $V_{2,3}$ and dorsal to the vestibular fenestra (according to Baumel et al. 1993) in *P. adeliae*, *P. antarctica* and *P. papua*. A small foramen appears in the three modern species, posterior to the CN VII foramen, which is not reconstructed in the endocasts, corresponding probably to a separate branch of this nerve. A third branch (probably the hyomandibular branch) is entering the tympanic cavity and is not visible in lateral view of the braincase.

Endocranially, there is a single foramen for all the branches of CN XII nerves, except in *P. adeliae*, which has two internal and three external foramina (Figures 8 and 9).

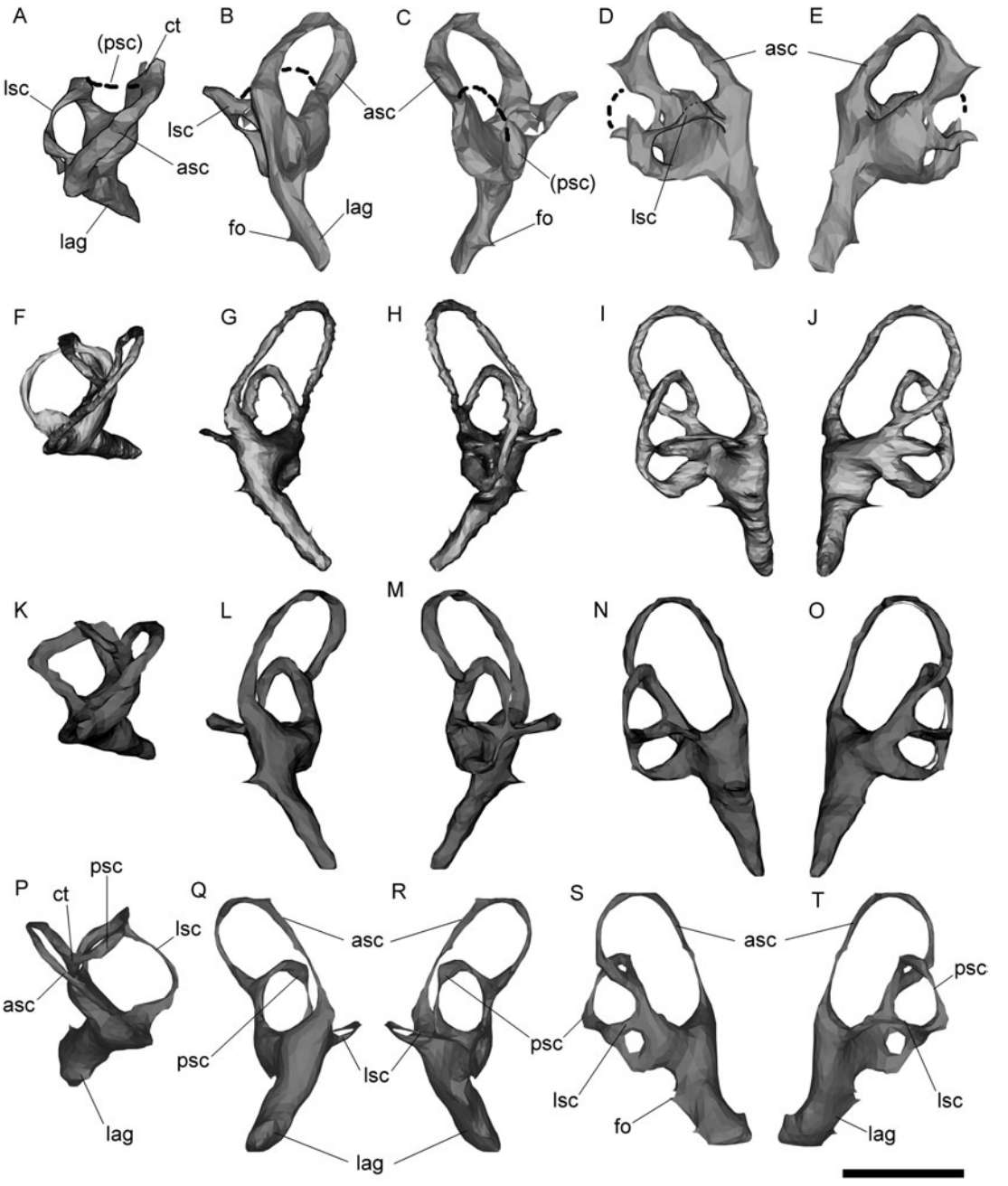

Figure 10. Digital reconstruction of the right inner ear of *P. calderensis* (A–E), *P. antarctica* (F–J) and *P. papua* (K–O), and left inner ear of *P. adeliae* (P–T) in dorsal (A, F, K, P), anterior (B, G, L, Q), posterior (C, H, M, R), lateral (D, I, N, S) and medial (E, J, O, T) views. asc, anterior semicircular canal; ct, common trunk; fo, fenestra ovalis; lag, lagena; lsc, lateral semicircular canal; psc, posterior semicircular canal. Scale bar = 1 cm.

The *vena occipitalis externa* opens dorsolaterally to the foramen magnum. Endocranially, the passage for this vascular element is slender and curved in the analysed specimens (Figure 9). The rostral middle cerebral vein is not observed on the endocast of *P. calderensis*. This vessel exits the endocranial cavity through a large fenestra within the rostral tympanic recess (Figures 3, 4 and 9). The dorsal head vein is not observed in the endocast, but probably it exits the endocranial cavity through the same foramen.

3.3 Inner ear morphology

The inner ear of the fossil *Paraptenodytes* and the extant penguin *P. antarctica* was described by Ksepka et al.

(2012). Here, we also include the description of the inner ear of *P. adeliae*, *P. papua* and fossil *P. calderensis* (Figure 10 and Table 1).

The inner ear of the *Pygoscelis* species has the general avian morphology with large and slender semicircular canals and a long and slender lagena. The orientation of the semicircular canals, particularly the anterior semicircular canal, and the lagena is oblique relative to the anteroposterior axis of the skull (e.g. Figure 10 (B),(C)). Among birds, the large and slender canals are related to presumed high manoeuvrability in *Archaeopteryx* and comparatively acrobatic flight in *Larus* and *Columba* (Milner and Walsh 2009). In the case of *Pygoscelis* species, it could be associated with diving skills.

In the fossil species *P. calderensis*, the semicircular canals are oval-shaped and slender (Figure 10(A)–(E)). The anterior semicircular canal is the largest of all, followed by the lateral semicircular canal and the posterior semicircular canal. The anterior semicircular canal is oval-shaped, markedly elongated dorsoventrally and with the main axis posteromedially oriented, as in the living species of *Pygoscelis*. It is also taller than the posterior semicircular canal. The enlargement and orientation of the anterior semicircular canal are also described for the fossil penguin *Paraptenodytes* (Ksepka et al. 2012) and are typical of birds, and supposed to enhance sensitivity to pitch movements (Gray 1955 in Ksepka et al. 2012).

The reconstructed lateral semicircular canal of *P. calderensis* is sub-circular in shape, as in the living species *P. adeliae* and *P. antarctica* (Figure 10(A),(F),(P)). Unlike them, *P. papua* has a lateral semicircular canal which has a rectangular anterior shape (Figure 10(K)). The anterior ampula is poorly developed in *P. calderensis* and *P. papua*, but is strongly developed in *P. adeliae* and *P. antarctica*, especially in the last taxon. In the fossil *Paraptenodytes*, the lateral semicircular canal is laterally projected surpassing the floccular lobe in dorsal view of the endocast, whereas in the extant *Pygoscelis*, *Aptenodytes* and *Spheniscus* the horizontal canal does not project as far laterally as the floccular lobe (Ksepka et al. 2012). This last is also true for the fossil *P. calderensis*. The posterior semicircular canal is also oval-shaped, although not markedly elongated as the anterior semicircular canal. The posterior section of the lateral semicircular canal contacts the posterior semicircular canal laterally, and the ventral section of the posterior semicircular canal is expanded ventrally to the lateral semicircular canal.

The common trunk is slender and the anterior and posterior semicircular canals are dorsally expanded over it. The lagena is simple (not coiled), long and conical, with a narrowed distal end. As in *Paraptenodytes* (Ksepka et al. 2012), and the living species of *Pygoscelis*, the lagena is oriented anteromedially and projects ventrally beyond the level of the medulla oblongata (Figures 6 and 8(B),(C)). The lagena is slightly more robust and shorter in *P. calderensis* and *P. adeliae* than in the other species. The length of this canal (cochlear canal) correlates highly with hearing range (Walsh et al. 2009), indicating that *P. calderensis* had a hearing sensitivity similar to that observed in living forms.

4. Final remarks and conclusions

Paleoneurological data are useful for varied paleobiological inferences. In fossil remains, this is the case for some brain structures (Witmer et al. 2003, 2008) and particularly the inner ear (Walsh et al. 2013). The comparison of the general morphology of extinct and extant *Pygoscelis* species shows that the olfactory bulbs, the *emimentia sagittalis*, optic lobes, floccular process and pituitary have approximately the same relative development (Figures 5–7). The brain similarity is consequent with the osseous and soft-tissue morphology, and these similarities are consequent with the related external morphology and with the ecological requirements known and inferred for each one of these taxa (Williams 1995; Acosta Hospitaleche and Tambussi 2006). Only subtle differences in the trophic habit could be observed between these living species (see Williams 1995 and references therein). The relationship between the external cranial morphology and diet preferences as well as the catching prey strategies were previously analysed (Acosta Hospitaleche and Tambussi 2006). As a result, a single morphotype was established for the three living *Pygoscelis* based on the *cristae nuchalis*, the *fossa temporalis* and the *fossa glandulae nasalis* configuration (Acosta Hospitaleche and Tambussi 2006; Acosta Hospitaleche 2011). Given that, it is not striking that brain morphology of the four species is similar. Because penguins capture prey while swimming, diving abilities are also partially related. Species that feed on krill, like *Pygoscelis*, would need less manoeuvrability under water than the piscivorous taxa (Haidr and Acosta Hospitaleche 2012). However, differences between *Pygoscelis* (crustacivores forms) are not evidenced in the auricular cerebelli and inner ear morphology when compared with *Spheniscus* or *Aptenodytes* (piscivorous forms). Given that most Eocene penguins were piscivorous (Acosta Hospitaleche 2013), crustacivory would have been a habit recently acquired along the history of the group. Therefore, the retention in *Pygoscelis* of inner ear characters is found in pursuit-diving penguins as *Aptenodytes* which are presumably related to their diving skills (Ksepka et al. 2012, Figure 7(E)), is not surprising.

Even when the brain of *P. calderensis* is similar in its morphology to the three living species of the genus, we arrived to important conclusions. The brain and inner ear pattern currently exhibited in *Pygoscelis* species was already present in the Mid-Miocene. The relative development of each sector of the brain suggests that the abilities and ecological requirements of the four species

would be at least similar, if not the same. For example, in extant and extinct penguins, the development of the wulst is similar to that in flying birds, indicating that this character was present before the loss of the flying capability (Ksepka et al. 2012). In *S. magellanicus*, for example, the wulst is three times larger than in the flightless tinamou (Bee de Speroni and Pirlot 1987). These authors suggest that the great development of the wulst is related to a sophisticated behaviour in penguins, which may have been the key factor of the adaptation and survival of the group since at least Paleocene times. On the other hand, the retention of this character of the wulst and other brain and inner ear features in *Pygoscelis* since the Miocene would also indicate that swimming manoeuvrability is a highly complex activity, equivalent to flying requirements.

Acknowledgements

The authors thank Dr D. Rubilar-Rogers (MNHN) and Dra. M. Picasso (MLP) for the access to the materials under their care. The authors thank the reviewers P. Jadwiszczak (Uniwersytet w Białymstoku, Poland) and RE Fordyce (Smithsonian Institution, USA), whose comments improved this manuscript. The authors also thank Agencia Nacional de Promoción Científica, Tecnológica and Consejo Nacional de Investigaciones Científicas y Técnicas (CONICET) (APC and CAH), and CONICYT (R.E. Y-Y) for constant support. Finally, the authors thank Dr A. Carlini (MLP) and B. Lafuente (Fundación Arturo López Pérez, Santiago) for the tomographies and Dr P. Currie (University of Alberta) for the access to the software used to create 3D models.

References

Achurra Reveco L. 2004. Cambios del nivel del mar y evolución tectónica de la cuenca Neógena de Caldera, III Región. Unpublished Magister Tesis. Santiago, Chile: Departamento de Geología de la Universidad de Chile.

Acosta Hospitaleche C. 2011. A new Patagonian penguin skull: taxonomic value of cranial characters. Ameghiniana. 48:605–620.

Acosta Hospitaleche C. 2013. New crania from Seymour Island (Antarctica) that shed light on anatomy of Eocene penguins. Pol. Polar Res. 34:397–412.

Acosta Hospitaleche C, Castro LN, Tambussi C, Scasso R. 2008. *Palaeospheniscus patagonicus* (Aves, Spheniscidae): new discoveries from the early Miocene of Argentina. J Palaeontol. 82 (3):565–575.

Acosta Hospitaleche C, Chavez M, Fritis O. 2006. Pingüinos fósiles (*Pygoscelis calderensis* sp.nov.) en la Formación Bahía Inglesa (Mioceno-Plioceno), Chile. Rev Geol Chile. 33(2):327–338.

Acosta Hospitaleche C, Tambussi C. 2006. Skull morphometry of *Pygoscelis* (Sphenisciformes): inter and intraspecific variations. Polar Biol. 29(9):728–734.

Acosta Hospitaleche C, Tambussi C, Donato M, Cozzuol MA. 2007. A new miocene penguin from Patagonia and its phylogenetic relationships. Acta Palaeontol Pol. 52(2):299–314.

Baumel JJ, King AS, Breazile JE, Evans HE. 1993. Handbook of avian anatomy: nomina anatomica avium. In: Baumel JJ, King AS, Breazile JE, Evans HE, Vanden Berge JC, editors. Publications of the nuttall ornithological club. 23, 779 pp.

Baumel JJ, Gerchman L. 1968. The avian carotid anastomosis. Am J Anat. 122:1–18.

Bee de Speroni N, Pirlot P. 1987. Relative size of avian brain components of the magellanic penguin, the greater *Rhea* and the Tataupa tinamou. Cormorant. 15:7–22.

Bertelli S, Giannini NP, Ksepka DT. 2006. Redescription and phylogenetic position of the early Miocene penguin *Paraptenodytes antarcticus* from Patagonia. Am Mus Novit. 3525:1–36.

Elzanowski A, Galton PM. 1991. Braincase of *Enaliornis*, an early Cretaceous bird from England. J Vertebr. Paleontol. 11:90–107.

Haidr N, Acosta Hospitaleche C. 2012. Feeding habits of Antarctic Eocene penguins from a morphofunctional perspective. N Jb Geol Paläont. 263(2):125–131.

Ksepka DT, Balanoff AM, Walsh S, Revan A, Ho A. 2012. Evolution of the brain and sensory organs in Sphenisciformes: new data from the stem penguin *Paraptenodytes antarcticus*. Zool J Linn. Soc. 166:202–219.

Marchant M, Marquardt C, Blanco N, Godoy E. 2000. Foraminíferos del área de Caldera (26°45′-28°S) y su utilización como indicadores cronoestratigráficos del Neógeno. In: Congreso Geológico Chileno, Puerto Varas. No. 9, Actas 1. p. 499–503.

Milner AC, Walsh SA. 2009. Avian brain evolution: new data from Palaeogene birds (Lower Eocene) from England. Zool J Linn. Soc. 155:198–219.

Rubilar-Rogers D, Otero R, Yury-Yáñez R, Vargas A, Gutstein C. 2012. An overview of the dinosaurs fossil record from Chile. J South Am Earth Sci. 37:242–255.

Saiff E. 1976. Anatomy of the middle ear region of the avian skull: Sphenisciformes. Auk. 93(4):749–759.

Simpson GG. 1972. Pliocene penguins from North Canterbury. Rec Canterbury Mus. 9(2):159–182.

Stucchi M. 2007. Los pingüinos de la Formación Pisco (Neógeno), Perú. In: Díaz–Martínez E, Rábano I, editors. 4th European Meeting on the Paleontology and Stratigraphy of Latin America, Cuadernos del Museo Geominero, no. 8 Madrid: Instituto Geológico y Minero de España; p. 367–373.

Walsh SA. 2001. The Bahía Inglesa Formation Bonebed: genesis and palaeontology of a Neogene Konzentrat Lagerstätte from north-central Chile. Unpublished PhD Thesis. University of Portsmouth.

Walsh SA, Barrett PM, Milner AC, Manley G, Witmer LM. 2009. Inner ear anatomy is a proxy for deducing auditory capability and behaviour in reptiles and birds. Proc R Soc. B. 276:1355–1360.

Walsh SA, Luo Z-X, Barret PM. 2013. Insights from comparative hearing research. In: Koppl C, et al., editors. Modern imaging techniques as a window to prehistoric auditory worlds. 49 Springer Handbook of Auditory Research, doi 10.1007/2506_2013_32.

Walsh SA, Milner A. 2011a. Evolution of the avian brain and senses. In: Dyke G, Kaiser G, editors. Living dinosaurs: the evolutionary history of modern birds. Chichester: Wiley; p. 282–305.

Walsh SA, Milner A. 2011b. *Halcyornis toliapicus* (Aves: Lower Eocene, England) indicates advanced neuromorphology in Mesozoic Neornithes. J Syst. Palaeontol. 9:173–181.

Walsh SA, Suárez M. 2006. New penguin remains from the Pliocene of Northern Chile. Hist Biol. 18:115–126.

Williams TD. 1995. The penguins. Oxford: Oxford University Press.

Witmer LM, Chatterjee S, Franzosa J, Rowe T. 2003. Neuroanatomy of flying reptiles and implications for flight, posture and behaviour. Nature. 425:950–953.

Witmer LM, Ridgely RC, Dufeau DL, Semones MC. 2008. Using CT to peer into the past: 3D visualisation of the brain and ear regions of birds, crocodiles and nonavian dinosaurs. In: Endo H, Frey R, editors. Anatomical imaging: towards a new morphology. Tokyo: Springer; p. 67–87.